

Goldstone mode and soft mode at the smectic-*A*—smectic-*C** phase transition studied by dielectric relaxation

A. Levstik, T. Carlsson,* C. Filipič, I. Levstik, and B. Žekš

J. Stefan Institute, E. Kardelj University of Ljubljana, 61111 Ljubljana, Jamova 39, Yugoslavia

(Received 17 November 1986)

The complex dielectric constant has been measured in a room-temperature ferroelectric liquid-crystal mixture. We have resolved the experimental data into the Goldstone mode and the soft mode and for each mode determined the dielectric strength and the corresponding relaxation frequency. The results are compared with the dielectric strength calculated using the extended Landau type of free-energy density proposed by Žekš [Mol. Cryst. Liq. Cryst. **114**, 259 (1984)], and it is shown that this calculation is able to describe the experimental data well. We have shown that by reasonable assumptions we can derive a simple relation between the Goldstone-mode contribution to the dielectric susceptibility (χ_2) and the polarization (P_0), tilt (θ_0), and pitch (p) of the system: $\chi_2 = (P_0 p / \theta_0)^2 / 8K_3 \pi^2$, where K_3 is a bend nematic curvature elastic constant. We also predict, on theoretical grounds, a small peak of the dielectric strength to exist at T_c .

I. INTRODUCTION

In 1975 the existence of ferroelectric liquid crystals was reported by Meyer *et al.*¹ Since then, considerable experimental and theoretical progress has been made in understanding the behavior of the smectic-*A*—smectic-*C** (Sm*A*-Sm*C**) transition. The temperature dependence of the tilt, the spontaneous polarization, and the pitch of the helix can be calculated to be in good agreement with experimental data if one, in the Landau expansion of the free-energy density, includes a biquadratic coupling as well as a bilinear one between tilt and polarization.^{2,3} In a recent work⁴ it is also shown by the authors how the dielectric susceptibility of Sm*C** liquid crystals can be calculated by this model. Here we will report high-resolution dielectric measurements of the room-temperature ferroelectric liquid crystal mixture 71.76 wt. % of 4-*n*-butyloxy-benzylidene-4'-*n*-octylaniline, 12.92 wt. % of 4-4'-bis-*n*-heptyloxy-azoxybenzene and 15.32 wt. % of 4''-(2-methylbutylphenyl)-4'-(2-methylbutyl)-4-biphenylcarboxylate (shortened by us to BAHABAC for convenience) close to the Sm*A*-Sm*C** transition. We also show how we are able to resolve the measured dielectric strength into the contributions from the soft mode and from the Goldstone mode. Comparing our experimental data with previous calculations^{5,6} of the static dielectric susceptibility of Sm*C** liquid crystals based on a relatively simple Landau expansion of the free-energy density, we will discuss how and why these calculations have failed to give a proper account of all the details of the experimental behavior of the system. We then show how an extended Landau type of free-energy density can be used⁴ to calculate the static dielectric susceptibility in fairly good agreement with the experimental data reported here. We also derive a simple expression relating the Goldstone-mode part of the dielectric susceptibility to the polarization, tilt, and pitch of the system.

II. DIELECTRIC PROPERTIES OF Sm*C** LIQUID CRYSTALS: GOLDSTONE MODE AND SOFT MODE

The chiral ferroelectric Sm*C** phase represents a spatially modulated structure.^{1,7,8} The tilt of the long molecular axis from the normal to the smectic layers precesses helicoidally as one goes from one smectic layer to another. The projection of the molecules into the smectic planes (which are taken to be parallel to the *xy* plane) is described by the order parameter $\xi = \xi_1 \hat{x} + \xi_2 \hat{y}$. Because of the chirality of the molecules the tilt locally breaks the axial symmetry around the long molecular axis and induces a transverse in-plane polarization $\mathbf{P} = P_x \hat{x} + P_y \hat{y}$ perpendicular¹ to the direction of the tilt (cf. Fig. 1). Denoting the wave vector of the helix by q we thus can write for small tilt angles

$$\xi_1 = \theta_0 \cos(qz), \quad \xi_2 = \theta_0 \sin(qz), \quad (1a)$$

$$P_x = -P_0 \sin(qz), \quad P_y = P_0 \cos(qz), \quad (1b)$$

where z is the coordinate normal to the smectic planes and θ_0 and P_0 are the magnitudes of the tilt angle and the spontaneous polarization of the system, respectively. Thus we see that even if the system exhibits a local net polarization, the macroscopic average of this will be zero. Applying an electric field of magnitude E parallel to the smectic layers will, however, disturb the helix in such a way that an average macroscopic polarization $\langle P_i \rangle$ is induced. The dielectric response χ is then defined as

$$\chi = \lim_{E \rightarrow 0} \langle P_i \rangle / E. \quad (2)$$

In order to calculate $\langle P_i \rangle$ in the limit of weak fields, we note that the electric field will disturb the helix in two ways. First of all the magnitude of the tilt of the molecules will change, and secondly the direction (phase) of

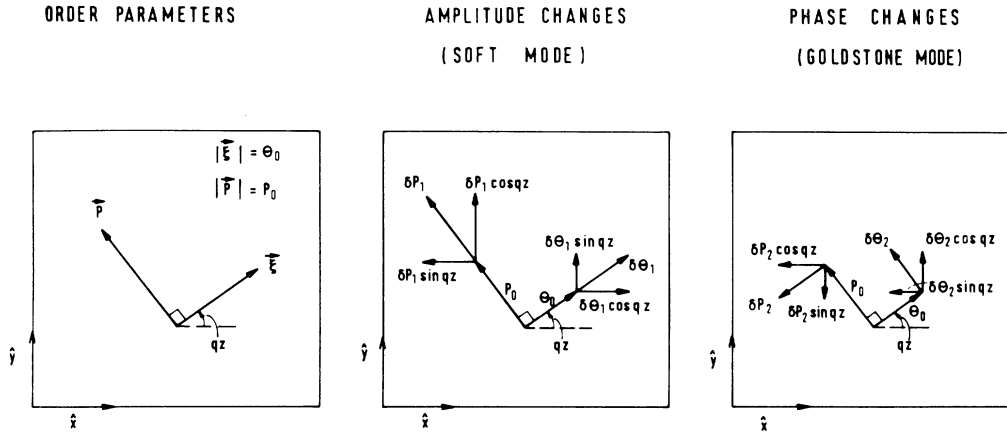


FIG. 1. Introduction of the order parameters ξ and \mathbf{P} and their changes due to the application of an electric field to the system. The amplitude changes, which are connected to the soft mode, are denoted $\delta\theta_1$ and δP_1 while the phase changes, which are connected to the Goldstone mode, are denoted $\delta\theta_2$ and δP_2 .

the tilt will rotate slightly in order to align the local polarization along the field. In this way both the amplitude and the phase of the order parameters ξ and \mathbf{P} will be influenced by the field. Denoting the amplitude changes by $\delta\theta_1$ and δP_1 and the phase changes by $\delta\theta_2$ and δP_2 , respectively, we see from Fig. 1 that ξ and \mathbf{P} can be written

$$\begin{aligned}\xi_1 &= \theta_0 \cos(qz) + \delta\theta_1 \cos(qz) - \delta\theta_2 \sin(qz), \\ \xi_2 &= \theta_0 \sin(qz) + \delta\theta_1 \sin(qz) + \delta\theta_2 \cos(qz), \\ P_x &= -P_0 \sin(qz) - \delta P_1 \sin(qz) - \delta P_2 \cos(qz), \\ P_y &= P_0 \cos(qz) + \delta P_1 \cos(qz) - \delta P_2 \sin(qz).\end{aligned}\quad (3)$$

By this ansatz we have divided the average induced polarization into two parts, $\langle P_i \rangle = \langle P_{i1} \rangle + \langle P_{i2} \rangle$, showing that the dielectric response separates into two modes, i.e., we can write $\chi = \chi_1 + \chi_2$. One part of χ is thus due to the amplitude changes of the polarization and is denoted the soft mode (χ_1) while the other part which is due to the phase changes of the polarization will be denoted the Goldstone mode⁹ (χ_2).

The general experimental behavior of the dielectric susceptibility will be discussed in the next section. What is usually experimentally determined is the dielectric strength defined by

$$\hat{\epsilon} = \epsilon_0 - \epsilon_\infty, \quad (4)$$

where ϵ_∞ and ϵ_0 are the infinite-frequency and static relative dielectric constants, respectively. The dielectric strength is related to the dielectric susceptibility χ by the relation

$$\chi = \epsilon_s \hat{\epsilon}, \quad (5)$$

where ϵ_s is the permittivity of free space.

Early calculations of χ presented by Martinot-Lagarde and Durand⁵ and by Benguigui⁶ have failed to in a proper way describe its experimental behavior. These two calculations are essentially identical and here we review the results of Ref. 5. Starting with a Landau expansion of the free-energy density in the presence of an electric field $\mathbf{E} = E\hat{\mathbf{x}}$ [the meaning of the terms entering g_0 will be discussed in connection with Eq. (11) in Sec. IV],

$$\begin{aligned}g_0(z) &= \frac{1}{2}a(\xi_1^2 + \xi_2^2) + \frac{1}{4}b(\xi_1^2 + \xi_2^2)^2 - \Lambda \left[\xi_1 \frac{d\xi_2}{dz} - \xi_2 \frac{d\xi_1}{dz} \right] + \frac{1}{2}K_3 \left[\left(\frac{d\xi_1}{dz} \right)^2 + \left(\frac{d\xi_2}{dz} \right)^2 \right] \\ &+ \frac{1}{2\epsilon}(P_x^2 + P_y^2) - \mu \left[P_x \frac{d\xi_1}{dz} + P_y \frac{d\xi_2}{dz} \right] + C(P_x \xi_2 - P_y \xi_1) - EP_x,\end{aligned}\quad (6)$$

they calculate the induced polarization in the limit of weak fields. For the SmC^* phase they ultimately arrive at the expression

$$\chi_{C^*} = \frac{1}{2} \left[\frac{C^2 \epsilon^2}{(K_3 - \epsilon \mu^2) q^2 + 2\alpha(T_c - T)} + \frac{C^2 \epsilon^2}{(K_3 - \epsilon \mu^2) q^2} \right], \quad (7)$$

where the two terms in the sum represent the contribution to χ from the soft mode and the Goldstone mode, respectively. T is the temperature of the system, T_c is the SmC^* - SmA phase transition temperature and q is the wave vector of the pitch

$$q = \frac{\epsilon \mu C + \Lambda}{K_3 - \epsilon \mu^2}. \quad (8)$$

As all material parameters entering Eq. (6) except a [$a = \alpha(T - T_0)$] are assumed to be temperature independent, q is constant within this model. Calculating χ in the Sm A phase, Martinot-Lagarde and Durand get

$$\chi_A = \frac{C^2 \epsilon^2}{(K_3 - \epsilon \mu^2) q^2 + \alpha(T - T_c)}, \quad (9)$$

a contribution which is solely attributed to the soft mode. The calculation thus predicts that the Goldstone mode should give a constant contribution to χ in all the Sm C^* phase while the soft mode contributes to χ only close to T_c , both in the Sm C^* phase and in the Sm A phase, showing a cusplike peak at T_c . At T_c both modes contribute equally. We shall see in the next section that this does not correctly describe the experimental behavior of χ . In Sec. IV we then show how we, by adding a few new terms to the free-energy density expansion, are able to calculate χ in good agreement with experiments.

III. EXPERIMENT

The mixture BAHABAC is in the ferroelectric helical Sm C^* phase at room temperature having a Sm A -Sm C^* phase transition temperature $T_c = 40.675^\circ\text{C}$. We have studied the temperature and frequency dependence of the complex dielectric constant ϵ^* perpendicular to the helical axis close to T_c . The sample was held between Nessa glass plates and the parallel orientation of the smectic planes was achieved by slowly cooling the sample in a magnetic field of 6.3 T from the isotropic phase. The measurements were performed after removing the sample from the magnet. An ac electric field was applied perpendicular to the normal of the smectic layers and the complex dielectric constant was measured in the frequency range from 20 Hz to 100 kHz keeping the temperature of the sample stable within $\pm 0.001^\circ\text{C}$. The results of these measurements have partly been published previously.¹⁰

As mentioned earlier we expect two relaxation modes to contribute to the dielectric behavior of ferroelectric liquid crystals. We thus can write the total dielectric strength as $\epsilon_0 - \epsilon_\infty = \Delta\epsilon_G + \Delta\epsilon_S$, where $\Delta\epsilon_G$ and $\Delta\epsilon_S$ represent the contributions from the two modes in question. The measured data were analyzed using a "generalized" Cole-Cole expression¹¹

$$\epsilon^*(\omega) - \epsilon_\infty = \sum_{i=G,S} \frac{\Delta\epsilon_i}{1 + (j\omega\tau_i)^{1-h_i}}, \quad (10)$$

where each term in the sum represents the contribution to the complex dielectric constant $\epsilon^* = \epsilon' - j\epsilon''$ from a separate dielectric mode. In Eq. (10) we have introduced the angular frequency of the applied electric field ω , the relaxation time of the i th mode $\tau_i = 1/2\pi f_i$, where f_i is the corresponding dispersion frequency, and the distribution parameter $h_i \in [0, 1]$. For each temperature the dielectric loss ϵ'' was corrected by subtracting $\epsilon''_1 = \sigma_1/\omega\epsilon_s$ which is the contribution from the low-frequency conductivity σ_1 (ϵ_s being the permittivity of free space). The experimental data were fitted to the expression of Eq. (10) varying the parameters $\Delta\epsilon_i$, ϵ_∞ , τ_i , h_i , and σ_1 . The values

of ϵ''_1 were, within 1%, equal to the ϵ'' measured at 20 Hz. In the Sm A phase, and in the Sm C^* phase except close to T_c , only one relaxation contributes and the sum of Eq. (10) consists of one term only. The corresponding characteristic frequency is then found to be the one where the dielectric loss ϵ'' adopts its maximum value.¹¹ Close to T_c , in the Sm C^* phase, however, both modes contribute to the dielectric response and the corresponding frequencies are obtained by fitting the sum of Eq. (10) to the experimental data. The distribution parameter h_i was everywhere found to be small.

In Fig. 2 the Cole-Cole diagrams at four different temperatures in the Sm C^* phase are shown. For the three lowest temperatures the results are described by Cole-Cole semicircles showing that only one relaxation behavior is present. As is discussed in Sec. II, the contribution to the dielectric constant from the soft mode is negligible in the Sm C^* phase except close to T_c . Thus this relaxation can be attributed to the Goldstone mode. At the temperature $T = 40.6^\circ\text{C}$, corresponding to $T_c - T = 0.075^\circ\text{C}$, the Cole-Cole diagram does not show up any longer as a pure semicircle. By fitting the expression of Eq. (10) to this distorted semicircle we can show that this Cole-Cole diagram is a superposition of two semicircles, i.e., at this temperature two modes are contributing to the dielectric response. Apart from the Goldstone mode we thus also observe a contribution from the soft mode if the measurements are performed sufficiently close to T_c . In the Sm A phase we were only able to perform measurements of ϵ^* in a narrow temperature interval just above T_c . Here the dielectric strength was observed to be 1 order of magnitude smaller than in the Sm C^* phase. The corresponding Cole-Cole diagrams of the measurements are shown in Fig. 3. Here we again observe only one relaxation behavior, which is attributed to the soft mode.

In Fig. 4 we have plotted the relaxation frequency of the Goldstone mode (triangles) and of the soft mode (crosses) obtained by the fitting. For $T > T_c$ the solid line through the experimental points is given by the expression $f_s = k(T - T_c)$ where we have determined k to be 15.6 kHz K^{-1} . The normal behavior of the soft mode in solid ferroelectrics is that the slope of the $f_s(T)$ line is twice as

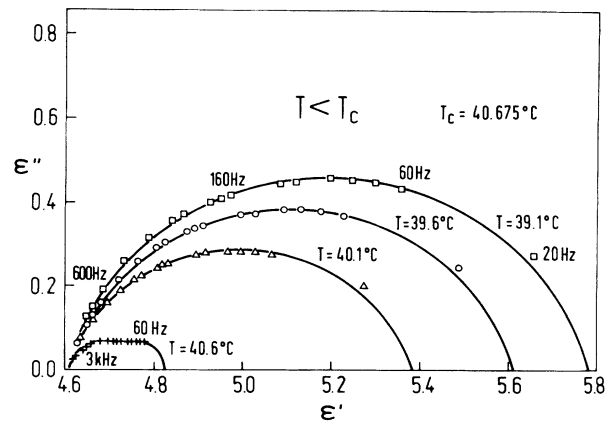


FIG. 2. Cole-Cole diagrams of BAHABAC at four different temperatures in the Sm C^* phase.

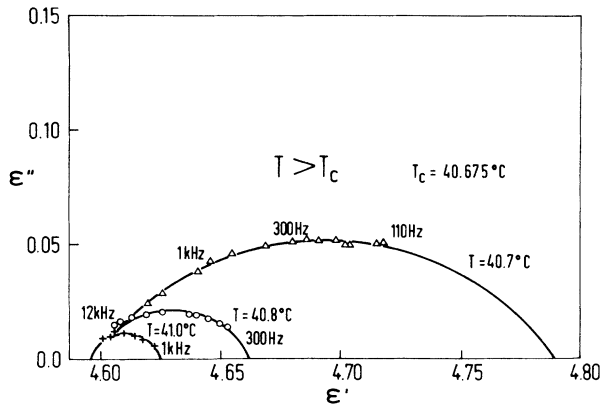


FIG. 3. Cole-Cole diagram of BAHABAC at three different temperatures in the Sm A phase.

large in the low symmetry phase.¹² Motivated by this we have plotted the line $f_s = 2k(T_c - T)$ for $T < T_c$ in Fig. 3. The solid line through the points of the Goldstone mode represents no fit but is just a guide to the eye. In addition to the two modes discussed above a high-frequency relaxation ~ 100 kHz was observed in the whole temperature range covered by the experiment.

In Fig. 5 the circles show the measured dielectric strength $\epsilon_0 - \epsilon_\infty$ as a function of temperature. We notice the maximum which is observed a few degrees below T_c . This is in accordance with what has been observed for *p*-decyloxybenzylidene-*p*'-amino-2-methylbutylcinnamate (DOBAMBC) by other authors.¹³⁻¹⁵ We will also point out that some authors^{6,16,17} locate this maximum to be situated at T_c . We believe that in these papers the location of T_c is wrong—these authors have probably assumed that the peak in the dielectric strength and T_c should coincide and have not determined T_c by any independent method. The solid line corresponding to the circles in Fig. 5 shows the result of the calculations of the dielectric strength which is presented below. This is the first calculation which is able to describe all the features of the ex-

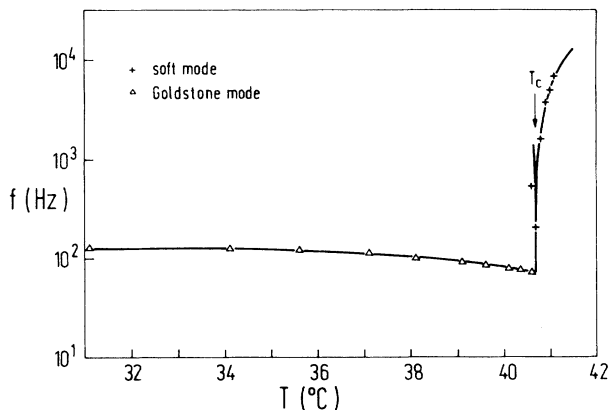


FIG. 4. The dielectric dispersion frequency of BAHABAC as a function of temperature.

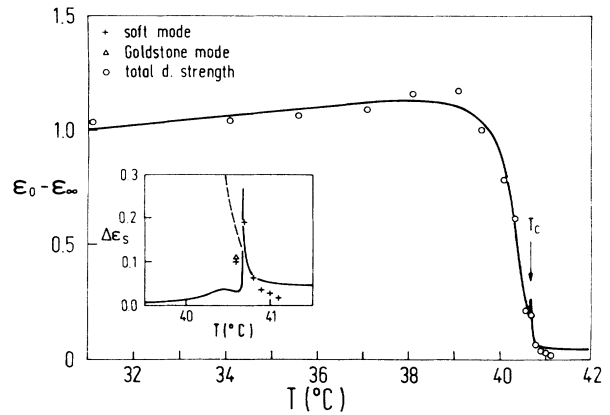


FIG. 5. The dielectric strength $\epsilon_0 - \epsilon_\infty$ of BAHABAC as a function of temperature (circles). The solid line represents the results of the calculations using the parameter values $\gamma = 2.08$, $\beta = 0.32$, $\rho = 0.036$, $\lambda = 0.14$, $\nu = -0.02$, and $\delta = 7.5 \times 10^{-3}$. The inset shows the separation of the dielectric strength into the Goldstone mode (triangles) and the soft mode (crosses). The solid line represents the calculated contribution of the soft mode while the dotted line represents the calculated contribution of the Goldstone mode.

perimental data correctly. We also note that the calculations indicate a small peak of the dielectric strength at T_c . In order to determine the experimental existence of this, high-resolution temperature measurements need to be performed close to T_c . In the measurements by Yoshino *et al.*¹³ there is, however, an indication of this peak's existence in the dielectric strength of DOBAMBC.

As is seen from the Cole-Cole diagram of Figs. 2 and 3 only one relaxation mechanism comes into play for each temperature except just below T_c . Only at $T = 40.6^\circ\text{C}$ do both modes contribute in such a way that it was possible to resolve the dielectric strength into its contributions from the Goldstone mode and the soft mode. This division is shown in the inset of Fig. 5, where the calculated contributions from the Goldstone mode (dotted line) and the soft mode (solid line) are shown separately. We note that both the experimental data as well as the calculations establish a finite contribution of the Goldstone mode at T_c . This is the first measurement where the contributions of the Goldstone mode and the soft mode to the dielectric response of ferroelectric liquid crystals have been presented separately. The soft mode was studied in DOBAMBC by Garoff and Meyer¹⁸ by measurements of the electrooptic response.

IV. THEORY

Comparing the predicted behavior^{5,6} of the dielectric susceptibility of ferroelectric liquid crystals which is a consequence of the free-energy density of Eq. (6) (cf. end of Sec. II) with the observed experimental behavior discussed in the preceding section (cf. Fig. 5) we note some discrepancies between theory and experiment. Motivated

by this we have in a recent work⁴ investigated the influence of adding a few more terms to the Landau expansion of the free-energy density of the system. By the use of this extended model we can, at the same time, calculate

$$g_0(z) = \frac{1}{2}a(\xi_1^2 + \xi_2^2) + \frac{1}{4}b(\xi_1^2 + \xi_2^2)^2 + \frac{1}{6}c(\xi_1^2 + \xi_2^2)^3 - \Lambda \left[\xi_1 \frac{d\xi_2}{dz} - \xi_2 \frac{d\xi_1}{dz} \right] + \frac{1}{2}K_3 \left[\left[\frac{d\xi_1}{dz} \right]^2 + \left[\frac{d\xi_2}{dz} \right]^2 \right] - d(\xi_1^2 + \xi_2^2) \left[\xi_1 \frac{d\xi_2}{dz} - \xi_2 \frac{d\xi_1}{dz} \right] + \frac{1}{2\epsilon}(P_x^2 + P_y^2) + \frac{1}{4}\eta(P_x^2 + P_y^2)^2 - \mu \left[P_x \frac{d\xi_1}{dz} + P_y \frac{d\xi_2}{dz} \right] + C(P_x\xi_2 - P_y\xi_1) - \frac{1}{2}\Omega(P_x\xi_2 - P_y\xi_1)^2, \quad (11)$$

where z is the coordinate normal to the smectic layers (which are taken to be parallel to the xy plane). Only the term quadratic in tilt is explicitly temperature dependent: $a = \alpha(T - T_0)$. K_3 is the elastic modulus, Λ the coefficient of the Lifshitz term responsible for the modulation, and μ and C are the coefficients of the flexoelectric and piezoelectric bilinear coupling. Ω is the coefficient of the biquadratic coupling term inducing transverse quadrupole ordering and the η term has been added to stabilize the system. The d term describes the monotonous increase of the pitch with temperature at low temperature. The sixth-order term in tilt (the c term) has been added to account for the specific-heat temperature dependence of the system.^{19,20} If an electric field is applied in the x direction, i.e., $\mathbf{E} = E\hat{x}$, this will give an additional contribution to the free-energy density

$$g_E(z) = -EP_x. \quad (12)$$

We have shown⁴ that the equations governing the behavior of the system which can be deduced from Eq. (11) are most conveniently studied by rewriting them into dimensionless form. By doing so we transform the 11 material parameters introduced in Eq. (11) to six independent dimensionless constants and five scaling factors. The six constants are defined as (the reader should please note that the set of constants we have chosen does not coincide with the choice which was made in the early version of this model presented in Ref. 3)

$$\gamma = \frac{\tilde{b}\eta}{\Omega^2}, \quad \beta = \frac{\eta^{1/2}\tilde{C}\tilde{\epsilon}}{\Omega^{1/2}}, \quad \rho = \frac{\tilde{c}\eta}{\tilde{\epsilon}\Omega^3}, \quad (13)$$

$$\lambda = \frac{\Lambda\eta^{1/2}\tilde{\epsilon}^{1/2}}{K_3^{1/2}\Omega^{1/2}}, \quad \nu = \frac{\mu\tilde{\epsilon}^{1/2}}{K_3^{1/2}}, \quad \delta = \frac{d\eta^{1/2}}{K_3^{1/2}\Omega^{3/2}\tilde{\epsilon}^{1/2}}, \quad (14)$$

where \tilde{a} , \tilde{b} , \tilde{c} , $\tilde{\epsilon}$, and \tilde{C} are renormalized constants given by

$$\tilde{a} = a - \frac{\Lambda^2}{K_3}, \quad \tilde{b} = b - \frac{4\Lambda d}{K_3}, \quad (14)$$

$$\tilde{c} = c - \frac{3d^2}{K_3}, \quad \frac{1}{\tilde{\epsilon}} = \frac{1}{\epsilon} - \frac{\mu^2}{K_3}, \quad \tilde{C} = C + \frac{\Lambda\mu}{K_3}.$$

the temperature dependence of the tilt, polarization, pitch, dielectric susceptibility, and heat capacity of the ferroelectric SmC* phase in qualitative accordance with experimental data. The free-energy density we use is given by

The physical quantities such as the polarization P_0 , the tilt θ_0 , the wave vector of the pitch q , and the dielectric susceptibility χ will now be expressed in dimensionless form and will be denoted by a tilde above the corresponding symbol, while the characteristic units with which these are measured will be denoted by an asterisk (e.g., $\tilde{\theta}_0 = \theta_0/\theta^*$). The reduced temperature, however, we denote by $\tau = (T_c - T)/T^*$. The characteristic units are chosen to be

$$\theta^* = \left[\frac{1}{\tilde{\epsilon}\Omega} \right]^{1/2}, \quad P^* = \left[\frac{1}{\tilde{\epsilon}\eta} \right]^{1/2}, \quad (15a)$$

$$q^* = \frac{1}{z^*} = \left[\frac{\Omega}{\eta\tilde{\epsilon}K_3} \right]^{1/2}, \quad \chi^* = \tilde{\epsilon}, \quad T^* = \frac{\tilde{b}}{\tilde{\epsilon}\alpha\Omega};$$

$$g^* = \frac{(P^*)^2}{\chi^*}, \quad c_p^* = \frac{(P^*)^2}{\chi^*T^*}, \quad E^* = \frac{P^*}{\chi^*}. \quad (15b)$$

The original 11 parameters [Eq. (11)] can thus be transformed into six dimensionless constants [Eqs. (13) and (14)], which determine the shape of the temperature dependences of the physical quantities, and into five characteristic units [Eq. (15a)]. The characteristic units of the free-energy density, of the heat capacity and of the electric field are not independent and are given in Eq. (15b) for completeness.

Introducing the ansatz of Eq. (1) of the order parameters into the free-energy density of Eq. (11) and eliminating q , this can be written in dimensionless form as

$$\tilde{g}_0 = \frac{1}{2}(\beta^2 - \gamma\tau)\tilde{\theta}_0^2 + \frac{1}{4}\gamma\tilde{\theta}_0^4 + \frac{1}{6}\rho\tilde{\theta}_0^6 + \frac{1}{2}\tilde{P}_0^2 - \beta\tilde{P}_0\tilde{\theta}_0 - \frac{1}{2}\tilde{P}_0^2\tilde{\theta}_0^2 + \frac{1}{4}\tilde{P}_0^4 - \nu\delta\tilde{P}_0\tilde{\theta}_0^3. \quad (16)$$

The equations for $\tilde{\theta}_0$ and \tilde{P}_0 are obtained by minimizing Eq. (16),

$$(\beta^2 - \gamma\tau)\tilde{\theta}_0 + \gamma\tilde{\theta}_0^3 + \rho\tilde{\theta}_0^5 - \tilde{\theta}_0\tilde{P}_0^2 - (\beta + 3\nu\delta\tilde{\theta}_0^2)\tilde{P}_0 = 0, \quad (17a)$$

$$\tilde{P}_0^3 + (1 - \tilde{\theta}_0^2)\tilde{P}_0 - (\beta + \nu\delta\tilde{\theta}_0^2)\tilde{\theta}_0 = 0, \quad (17b)$$

while \tilde{q} [obtained by minimizing Eq. (16) before the substitution] is given by

$$\tilde{q} = \lambda + \nu \tilde{P}_0 / \tilde{\theta}_0 + \delta \tilde{\theta}_0^2. \quad (18)$$

While the tilt, polarization, and pitch are given straightforwardly by solving Eqs. (17) and (18), the dielectric susceptibility which is defined by Eq. (2) has yet to be determined. By substituting the ansatz (3) of the disturbed helix into Eqs. (11) and (12) the free-energy density

can be written as $\tilde{g} = \tilde{g}_0 + \tilde{g}_E(\tilde{z}) + \tilde{g}_2(\tilde{z})$ where \tilde{g}_0 is already given by Eq. (16), and $\tilde{g}_E(\tilde{z})$ is the part proportional to the electric field

$$\tilde{g}_E(\tilde{z}) = \tilde{E}[\tilde{P}_0 \sin(\tilde{q}\tilde{z}) + \delta \tilde{P}_1 \sin(\tilde{q}\tilde{z}) + \delta \tilde{P}_2 \cos(\tilde{q}\tilde{z})] \quad (19)$$

and $\tilde{g}_2(\tilde{z})$ is the part which is quadratic in the changes $\delta \tilde{\theta}_1$, $\delta \tilde{\theta}_2$, $\delta \tilde{P}_1$, and $\delta \tilde{P}_2$:

$$\begin{aligned} \tilde{g}_2(\tilde{z}) = & \delta \tilde{\theta}_1^2 [\frac{1}{2} \beta^2 - \frac{1}{2} \gamma \tau + \frac{3}{2} \gamma \tilde{\theta}_0^2 + \frac{5}{2} \rho \tilde{\theta}_0^4 + \frac{1}{2} \nu^2 (\tilde{P}_0 / \tilde{\theta}_0)^2 + 2\delta^2 \tilde{\theta}_0^4 - 5\nu \delta \tilde{P}_0 \tilde{\theta}_0 - \frac{1}{2} \tilde{P}_0^2] \\ & + \delta \tilde{\theta}_2^2 [\frac{1}{2} \beta^2 - \frac{1}{2} \gamma \tau + \frac{1}{2} \gamma \tilde{\theta}_0^2 + \frac{1}{2} \rho \tilde{\theta}_0^4 + \frac{1}{2} \nu^2 (\tilde{P}_0 / \tilde{\theta}_0)^2 - \nu \delta \tilde{P}_0 \tilde{\theta}_0] + \delta \tilde{P}_1^2 (\frac{1}{2} + \frac{1}{2} \nu^2 - \frac{1}{2} \tilde{\theta}_0^2 + \frac{3}{2} \tilde{P}_0^2) \\ & + \delta \tilde{P}_2^2 (\frac{1}{2} + \frac{1}{2} \nu^2 + \frac{1}{2} \tilde{P}_0^2) - \delta \tilde{\theta}_1 \delta \tilde{P}_1 (\nu^2 \tilde{P}_0 / \tilde{\theta}_0 + \nu \delta \tilde{\theta}_0^2 + \beta + 2\tilde{P}_0 \tilde{\theta}_0) - \delta \tilde{\theta}_2 \delta \tilde{P}_2 (\nu^2 \tilde{P}_0 / \tilde{\theta}_0 + \nu \delta \tilde{\theta}_0^2 + \beta + \tilde{P}_0 \tilde{\theta}_0) \\ & + \delta \tilde{\theta}_1 \delta \tilde{\theta}_2 (\nu \tilde{P}_0 / \tilde{\theta}_0 - 2 \delta \tilde{\theta}_0^2) - \delta \tilde{\theta}_1' \delta \tilde{\theta}_2 \nu \tilde{P}_0 / \tilde{\theta}_0 + \frac{1}{2} (\delta \tilde{\theta}_1'^2 + \delta \tilde{\theta}_2'^2) - \nu \delta \tilde{P}_1 \delta \tilde{\theta}_2' + \nu \delta \tilde{P}_2 \delta \tilde{\theta}_1'. \end{aligned} \quad (20)$$

A prime in Eq. (20) denotes a derivative with respect to the \tilde{z} coordinate. We now want to find the configuration of the system which minimizes the total free energy. By applying the Euler-Lagrange equations we derive four coupled second-order differential equations determining the four unknowns [$\delta \tilde{\theta}_1(\tilde{z})$, $\delta \tilde{\theta}_2(\tilde{z})$, $\delta \tilde{P}_1(\tilde{z})$, and $\delta \tilde{P}_2(\tilde{z})$] in such a way that $\tilde{g}_2(\tilde{z}) + \tilde{g}_E(\tilde{z})$ is minimized and the averaged (with respect to \tilde{z}) induced polarization $\langle \tilde{P}_i \rangle$ can thus be calculated. The dielectric response is then given by Eq. (2). The derivation of the resulting expression has been presented by us elsewhere.⁴ Separating $\tilde{\chi}$ into its contributions from the soft mode $\tilde{\chi}_1$, and the Goldstone mode $\tilde{\chi}_2$, the resulting expressions are given by

$$\tilde{\chi}_1 = (-\tilde{b}_1 \tilde{b}_4 \tilde{b}_6 + \tilde{b}_1 \tilde{b}_5 \tilde{b}_8 + \tilde{b}_1 \tilde{b}_6^2 + \tilde{b}_2 \tilde{b}_3 \tilde{b}_6 + \tilde{b}_2 \tilde{b}_4^2 - 2\tilde{b}_2 \tilde{b}_4 \tilde{b}_6 - \tilde{b}_2^2 \tilde{b}_8 - \tilde{b}_3 \tilde{b}_4 \tilde{b}_5 + \tilde{b}_4^2 \tilde{b}_5) / 2A, \quad (21a)$$

$$\tilde{\chi}_2 = (\tilde{b}_1 \tilde{b}_4^2 - \tilde{b}_1 \tilde{b}_4 \tilde{b}_6 + \tilde{b}_1 \tilde{b}_5 \tilde{b}_7 - 2\tilde{b}_2 \tilde{b}_3 \tilde{b}_4 + \tilde{b}_2 \tilde{b}_3 \tilde{b}_6 + \tilde{b}_2 \tilde{b}_4^2 - \tilde{b}_2^2 \tilde{b}_7 - \tilde{b}_3 \tilde{b}_4 \tilde{b}_5 + \tilde{b}_3^2 \tilde{b}_5) / 2A. \quad (21b)$$

The quantity A entering Eqs. (21) is defined as

$$\begin{aligned} A = & \tilde{b}_1 \tilde{b}_4^2 \tilde{b}_8 + \tilde{b}_1 \tilde{b}_5 \tilde{b}_7 \tilde{b}_8 + \tilde{b}_1 \tilde{b}_6^2 \tilde{b}_7 - 2\tilde{b}_2 \tilde{b}_3 \tilde{b}_4 \tilde{b}_8 \\ & - 2\tilde{b}_2 \tilde{b}_4 \tilde{b}_6 \tilde{b}_7 - \tilde{b}_2^2 \tilde{b}_7 \tilde{b}_8 - 2\tilde{b}_3 \tilde{b}_4^2 \tilde{b}_6 + \tilde{b}_3^2 \tilde{b}_5 \tilde{b}_8 \\ & + \tilde{b}_3^2 \tilde{b}_6^2 + \tilde{b}_4^4 + \tilde{b}_4^2 \tilde{b}_5 \tilde{b}_7 \end{aligned} \quad (22)$$

and the coefficients \tilde{b}_i ($i = 1-8$) are given by

$$\begin{aligned} \tilde{b}_1 = & -\beta^2 + \gamma \tau - \lambda^2 - (2\lambda \delta + 3\gamma) \tilde{\theta}_0^2 - 5\rho \tilde{\theta}_0^4 \\ & + \tilde{P}_0^2 + 8\nu \delta \tilde{P}_0 \tilde{\theta}_0 - 2\lambda \nu \tilde{P}_0 / \tilde{\theta}_0 - 2\nu^2 (\tilde{P}_0 / \tilde{\theta}_0)^2 - 5\delta^2 \tilde{\theta}_0^4, \\ \tilde{b}_2 = & -2\lambda \delta \tilde{\theta}_0^2 - 2\delta^2 \tilde{\theta}_0^4 + 2\lambda \nu \tilde{P}_0 / \tilde{\theta}_0 + 2\nu^2 (\tilde{P}_0 / \tilde{\theta}_0)^2, \\ \tilde{b}_3 = & \beta + \nu \delta \tilde{\theta}_0^2 + 2\tilde{P}_0 \tilde{\theta}_0 + \nu^2 \tilde{P}_0 / \tilde{\theta}_0, \\ \tilde{b}_4 = & -(\lambda \nu + \nu^2 \tilde{P}_0 / \tilde{\theta}_0 + \nu \delta \tilde{\theta}_0^2), \\ \tilde{b}_5 = & -\beta^2 + \gamma \tau - \lambda^2 - (2\lambda \delta + \gamma) \tilde{\theta}_0^2 - \rho \tilde{\theta}_0^4 \\ & - \delta^2 \tilde{\theta}_0^4 - 2\lambda \nu \tilde{P}_0 / \tilde{\theta}_0 - 2\nu^2 (\tilde{P}_0 / \tilde{\theta}_0)^2, \end{aligned} \quad (23)$$

$$\tilde{b}_6 = \beta + \nu \delta \tilde{\theta}_0^2 + \tilde{P}_0 \tilde{\theta}_0 + \nu^2 \tilde{P}_0 / \tilde{\theta}_0,$$

$$\tilde{b}_7 = 1 + \nu^2 + 3\tilde{P}_0^2 - \tilde{\theta}_0^2,$$

$$\tilde{b}_8 = 1 + \nu^2 + \tilde{P}_0^2.$$

Concerning the dielectric susceptibility in the Sm A phase the following expression is derived:

$$\chi_A = \frac{\beta^2 + \lambda^2 - \gamma \tau}{(1 + \nu^2)(\beta^2 + \lambda^2 - \gamma \tau) - (\beta - \lambda \nu)^2}. \quad (24)$$

With the exception of the constant high-temperature part which is included in our Eq. (24), this expression can be shown to be the same as that derived by Martinot-Lagarde and Durand [Eq. (9)]. That the two models give the same result in the Sm A phase is due to the fact that here the extra terms introduced by our extended version of the free-energy density only contribute to fourth order in $\delta \tilde{\theta}$ and $\delta \tilde{P}$. Such terms do not enter the calculation of $\tilde{\chi}$.

By the use of Eqs. (4) and (5) we are now able to compare the calculated $\tilde{\chi}$ with the measured dielectric strength $\epsilon_0 - \epsilon_\infty$. Into the calculations the six dimensionless parameters defined by Eqs. (13) and (14) and two scaling factors T^* and χ^* enter. The curve in Fig. 5 represents the best fit through the measured values using the parameters $\gamma = 2.08$, $\beta = 0.32$, $\rho = 0.036$, $\lambda = 0.14$, $\nu = -0.02$, and $\delta = 7.5 \times 10^{-3}$. The scaling factors have been chosen to be $T^* = 0.52$ K and $\chi^* = 3.7 \times 10^{-13}$ C/V m.

V. DISCUSSION

As discussed previously there are two different relaxation mechanisms which contribute to the dielectric strength of ferroelectric liquid crystals. One of those is connected to the phase changes (Goldstone mode) while the other one is connected to the amplitude changes (soft mode) of the order parameters. The Goldstone mode gives a finite contribution in all of the Sm C^* phase, showing a drop but still being finite as T_c is approached. In the Sm A phase the Goldstone mode is absent. The soft mode is present in both the Sm C^* and the Sm A phases

but is suppressed to negligible values in the SmC^* phase except close to T_c , a fact which makes it hard to resolve with respect to the Goldstone mode as $T_c - T$ gets too large. In the SmA phase the soft mode is rapidly suppressed to its limiting value $\tilde{\chi}_A(|\tau| \rightarrow \infty) = 1/(1 + \nu^2)$, which is written $\chi_A(T \rightarrow \infty) = \epsilon$ in physical units. At T_c our calculations show that the two modes contribute equally to $\tilde{\chi}$, a behavior which is also experimentally observed as can be seen in the inset of Fig. 5. We thus conclude that our theoretical model not only gives a good description of the total dielectric response of ferroelectric liquid crystals but also of the contribution from the Goldstone mode and the soft mode separately. We also conclude that the maximum of χ which is generally observed in ferroelectric liquid crystals^{6,13-17} is located a few degrees below T_c . In addition to this, our calculations indicate a small finite peak of χ at T_c in accordance to what was observed by Yoshino *et al.*¹³ Similar results to those reported above have also been observed by us in DOBAMBC.²¹

When writing down the extended Landau expansion of the free-energy density [Eq. (11)] we introduced altogether 11 material parameters. This is a large number, but by the introduction of the renormalized, dimensionless constants [Eqs. (13) and (14)] we have reduced the number of independent parameters to six. We also want to stress that the model is not only used to calculate the dielectric response, but also the polarization, the tilt, the pitch, and the heat capacity of the system.⁴ This means that we use six parameters to calculate the temperature dependence of five experimentally observed quantities (or six if one takes the separation of χ into the Goldstone mode and the soft mode into account).

In order to get a feeling for the meaning of the six constants we note that they appear in the calculations on different levels. As we have found $\nu\delta$ to be several orders of magnitude smaller than the parameters γ , β , and ρ , we note from Eqs. (17) that only the last three parameters effectively enter the calculation of the tilt and the polarization of the system. The ρ term ($\rho = c\eta/\epsilon\Omega^3$), being present due to the introduction of the $c\theta^6$ term in the free-energy density, does not introduce any qualitatively new features to the solution of Eqs. (17) but merely gives saturation effects at large θ_0 and P_0 . The ρ term is present in order to account for, in a proper way, the bent shape of the heat capacity of the SmC^* phase.^{19,20} Thus only the parameters γ and p are needed in order to, in a qualitatively correct way, describe the tilt and the polarization of the system while ρ has to be included if one also wants to correctly describe the heat capacity qualitatively. One can see from the definition of Eqs. (13) that the parameter β reflects the relative importance of the bilinear coupling (the C term) and the biquadratic coupling (the Ω term) between tilt and polarization in the free-energy density of Eq. (11). The shape of the graph of the polarization versus temperature is also critically dependent on this parameter.⁴ When β exceeds a value of approximately 0.5 (bilinear coupling dominating) the polarization curve exhibits a classical square-root behavior. If, on the hand, β is less than 0.5 (biquadratic coupling dominating) the polarization curve exhibits a sigmoidal (S -shaped) behavior

characterized by one square-root behavior close to T_c and another one far from T_c .

As is seen from Eq. (18) the parameters λ , ν , and δ have to be included into the calculation if one wants to, in a proper way, take into account the temperature dependence of the pitch. The λ term ($\lambda = \Lambda\eta^{1/2}\epsilon^{-1/2}/K_3^{1/2}\Omega^{1/2}$) is connected to the Lifshitz term (the Λ term) and would alone give rise to a temperature-independent pitch and so the ν and δ terms have to be introduced to, in a correct way, describe the temperature dependence of the pitch. The δ term is the one responsible for the decrease of the pitch at low temperatures (i.e., when $T_c - T$ gets large). Also, as can be deduced from Eqs. (21)–(23), the constants λ , ν , and δ are of the utmost importance when calculating the dielectric response of the system.

We finally discuss how we can get a physical understanding of the dependence of the dielectric susceptibility in terms of the quantities tilt, polarization, and pitch. Concerning the soft mode, one can show²⁰ that the amplitudes of the order parameters are affected by external forces only when close to T_c . This explains why the contribution of the soft mode is rapidly suppressed far away from T_c while in the vicinity of T_c it contributes in a cusplike way. Still, however, no critical divergence of the soft mode is expected. This is due to the fact that at T_c the SmA phase becomes unstable with respect to helicoidal fluctuations with wave vector $2\pi/p(T_c)$, while in dielectric measurements a homogeneous external field couples to $q=0$ fluctuations above T_c and to $q=0$ and $q=4\pi/p$ fluctuations below T_c . Only the response of the system with respect to a modulated external field ($q_E = 2\pi/p$) can be infinite. Concerning the Goldstone mode we make the following reasoning. The coupling of \mathbf{P} to the external field increases with P_0 . This suggests $\chi_2 \sim P_0^2$ as the response cannot depend on the sign of P_0 .

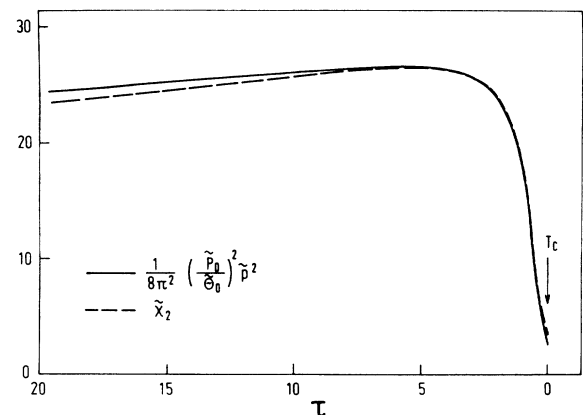


FIG. 6. The calculated contribution of the Goldstone mode to the dielectric susceptibility (dashed line) is compared to the calculated ratio $(\tilde{P}_0 \tilde{p} / \tilde{\theta}_0)^2 / 8\pi^2$ (solid line) as function of reduced temperature. The similarity of the two curves supports the hypothesis that the Goldstone-mode contribution to the dielectric susceptibility of ferroelectric liquid crystals is proportional to the square of the pitch times the square of the ratio of the polarization and the tilt.

Furthermore, the elastic energy associated by the pitch is given by $g_K = K_3 q^2 \theta_0^2 / 2$. This suggests $\chi_2 \sim 1 / K_3 q^2 \theta_0^2$. Altogether we thus expect the Goldstone-mode part of the dielectric susceptibility to obey $\chi_2 \sim P_0^2 p^2 / K_3 \theta_0^2$, a relation which is also dimensionally correct. The missing numerical factor in this relation can be derived⁴ to be $1/8\pi^2$. We thus predict the following approximative behavior of χ_2 :

$$\chi_2 = \frac{1}{8\pi^2 K_3} \left[\frac{P_0 p}{\theta_0} \right]^2, \quad (25a)$$

$$\tilde{\chi}_2 = \frac{1}{8\pi^2} \left[\frac{\tilde{P}_0 \tilde{p}}{\tilde{\theta}_0} \right]^2, \quad (25b)$$

where the relation is given both in physical and dimensionless units. In order to verify the validity of Eq. (25b), in Fig. 6 we have plotted the Goldstone-mode contribution of the dielectric susceptibility χ_2 calculated by the use of the parameters given at the end of Sec. IV (dashed line). In the same figure is also plotted $(\tilde{P}_0 \tilde{p} / \tilde{\theta}_0)^2 / 8\pi^2$ calculated by the same parameters. We notice that the two curves almost fall on top of each other. We have also checked the relation by performing numerous calculations for different sets of parameters. For each calculation the numerical constant which enters Eq. (25b) was found to de-

viate less than 10^{-4} from the value $1/8\pi^2$. As we have not performed any measurements of the polarization of BAHABAC, we cannot verify the experimental validity of Eq. (25a) in this case. We have, however, calculated⁴ $(P_0 p / \theta_0)^2 / 8\pi^2 \chi_2$ from experimental data obtained for DOBAMBC. This ratio, which should equal K_3 , was found to be constant within the experimental uncertainty and approximately equal to 3.8×10^{-12} N. This value is roughly what one would expect for the elastic constant of DOBAMBC. This verifies that the relations (25) give a good approximation of the Goldstone-mode contribution to the dielectric susceptibility of ferroelectric liquid crystals. It is thus easy to understand why the calculation of χ based on the free-energy density given by Eq. (6) fails to describe the temperature dependence properly. This model predicts⁵ both q and P_0/θ_0 to be temperature independent. It is thus necessary to extend the free-energy density in such a way that a more realistic prediction of q as well as of P_0/θ_0 is given. This is done by the extended free-energy density which we introduce in Eq. (11).

ACKNOWLEDGMENTS

We are indebted to J. W. Doane for kindly sending us a sample of BAHABAC at an early stage of this work.

*On leave of absence from the Institute of Theoretical Physics, Chalmers University of Technology, S-412 96 Göteborg, Sweden.

¹R. B. Meyer, L. Liebert, L. Strzelecki, and P. J. Keller, *J. Phys. (Paris) Lett.* **36**, L69 (1975).

²B. Žekš, *Mol. Cryst. Liq. Cryst.* **114**, 259 (1984).

³C. Filipič, A. Levstik, I. Levstik, R. Blinc, B. Žekš, M. Glogarova, and T. Carlsson, *Ferroelectrics* (to be published).

⁴T. Carlsson, B. Žekš, C. Filipič, A. Levstik, and R. Blinc (unpublished).

⁵Ph. Martinot-Lagarde and G. Durand, *J. Phys. (Paris) Lett.* **41**, L43 (1980).

⁶L. G. Benguigui, *Ferroelectrics* **58**, 269 (1984).

⁷S. A. Pikin and V. L. Indenbom, *Usp. Fiz. Nauk* **125**, 251 (1978).

⁸R. Blinc and B. Žekš, *Phys. Rev. A* **18**, 740 (1978).

⁹This separation which is done with respect to the polarization is only approximate. The part which corresponds to the amplitude change in \mathbf{P} mostly corresponds to the amplitude changes in ξ , but also includes a small phase contribution in the tilt because of a small amplitude-phase coupling. We have, however, proved in Ref. 4 that this coupling is so weak

that no significant changes of the results of the calculations presented below will appear in a more rigorous treatment.

¹⁰A. Levstik, B. Žekš, C. Filipič, R. Blinc, and I. Levstik, *Ferroelectrics* **58**, 33 (1984).

¹¹K. S. Cole and R. H. Cole, *J. Chem. Phys.* **9**, 341 (1941).

¹²R. Blinc and B. Žekš, *Soft Modes in Ferroelectrics and Antiferroelectrics* (North-Holland, Amsterdam, 1974).

¹³K. Yoshino, T. Uemato, and Y. Inuishi, *Jpn. J. Appl. Phys.* **16**, 571 (1977).

¹⁴A. Levstik, B. Žekš, I. Levstik, R. Blinc, and C. Filipič, *J. Phys. (Paris) Colloq.* **40**, C3-303 (1979).

¹⁵M. Glogarova and J. Pavel, *Mol. Cryst. Liq. Cryst.* **114**, 249 (1984).

¹⁶J. Hoffman, W. Kuczynski, and J. Malecki, *Mol. Cryst. Liq. Cryst.* **44**, 287 (1978).

¹⁷B. I. Ostrowski, A. Z. Rabinovich, A. S. Sonin, and B. A. Strukov, *Zk. Eksp. Teor. Fiz.* **74**, 1748 (1978).

¹⁸S. Garoff and R. B. Meyer, *Phys. Rev. Lett.* **38**, 848 (1977).

¹⁹C. C. Huang and J. M. Viner, *Phys. Rev. A* **25**, 3385 (1982).

²⁰T. Carlsson and I. Dahl, *Mol. Cryst. Liq. Cryst.* **95**, 373 (1983).

²¹A. Levstik, T. Carlsson, C. Filipič, and B. Žekš (unpublished).